SOLIDIFICATION STRUCTURES DURING LASER TREATMENT

Hegge, H.J.; Hosson, J.Th.M. De

Published in:
Scripta Metallurgica et Materialia

DOI:
10.1016/0956-716X(90)90207-W

Publication date:
1990

Scripta METALLURGICA et MATERIALIA
Vol. 24, pp. 593-599, 1990
Printed in the U.S.A.

SOLIDIFICATION STRUCTURES DURING LASER TREATMENT

H. J. Hegge, J. Th. M. De Hosson

Department of Applied Physics, Materials Science Centre,
University of Groningen, Nijenborgh 18, 9747 AG Groningen, The Netherlands

(Received November 28, 1989)
(Revised January 17, 1990)

Introduction

Most of the beneficial effects of a laser treatment, e.g. high hardness [1], good corrosion properties [2] and wear behaviour [3] can be attributed to specific solidification structures. In this paper attention is paid to the solidification structures resulting from a laser treatment and their relation to the conditions in a laser melt bath.

Important features determined during solidification are the type, the size and the distribution of the microstructure [4]. Those depend mainly on the velocity of the solidification front, the temperature gradient and the concentration of the various constituents [5]. As a result a flat solidification front, a cellular, a dendritic or an eutectic front may exist producing a specific solidification pattern. Although in general these features can be understood with existing theories, a considerable debate exists on detailed questions [6] [7].

In a laser treatment high solidification velocities (0.01-1 m/s) and high temperature gradients (10^4-10^6 K/m) are found, so that this process can be regarded as situated between welding and splat cooling. It is commonly known about a laser treatment that a fine, usually a cellular/dendritic structure [8] is formed, sometimes with a higher solid solubility of alloying elements [9]. To obtain more insight into which solidification phenomena attention is focussed here on Al-Si alloys, a type of alloy often used for casting. A disadvantage of this system might be the anisotropic interface between Al and Si, which plays an important role in eutectic solidification [5]. Alloys with varying concentrations Si are studied with a range of laser beam velocities in order to make solidification maps and to compare experimental results with theory.

Experiment

In this investigation four Al-Si alloys were studied: Al-4Si, Al-7Si, Al-12Si (eutectic) and Al-20Si. The specimens were ground blasted to get a rough surface, which absorbed well the laser light used (wavelength 10.6 μm). After sand blasting the samples were ultrasonically cleaned. The specimens were mounted on a numerically controlled X-Y table and irradiated by a 1.5 kW CO_2 Spectra Physics 820 laser. The Gaussian beam was deflected by a Mo mirror and focussed by a ZnSe lens before it impinges on the surface. At the surface the power of the beam was 1300 W. The focus point of the lens lay 5 mm above the surface. A separation of the different passes of approximately 5 mm provided that there was no effect of adjacent passes by the next one. The scanning velocities were between 1 and 25 cm/s.

After the laser treatment cross sectional samples were prepared for hardness measurements, optical (OM) and scanning electron microscopy (SEM). Microscopic studies were performed to measure the cellular/dendritical widths.

Results

After a laser treatment with different laser scan velocities (0.1-25 cm/s) cross sections were made of four different alloys: Al-4Si, Al-7Si, Al-12Si (± eutectic), Al-20Si.

At each velocity and concentration the type of structure was identified in the middle of the laser pass and structural maps (Fig. 1) were made.

0036-9748/90 $3.00 + .00

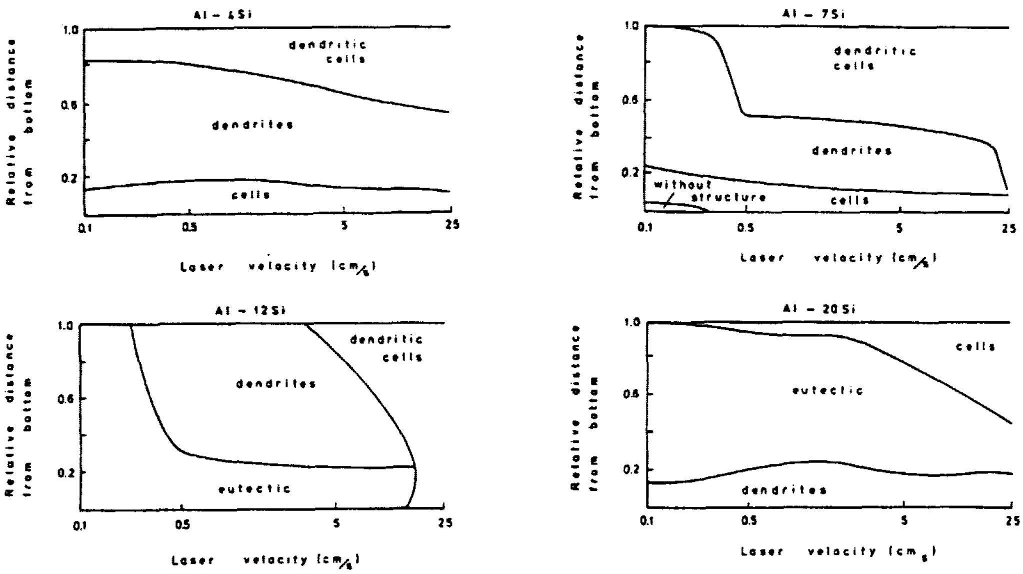

Fig. 1 *Solidification maps of Al-4Si, Al-7Si, Al-12Si, Al-20Si: structure in the middle of the melt bath vs. laser scan velocity (0 = bottom melt bath, 1 = top melt bath).*

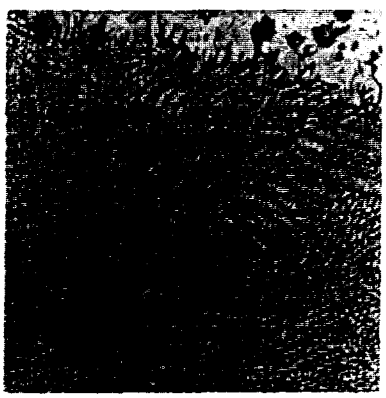

Fig. 2 *(Left) Cross section of Al-7Si after laser treatment (scan velocity 1 cm/s).*
Fig. 3 *(Right) Microstructure of Al-7Si after laser treatment (scan velocity 10 cm/s).*

A typical example for hypo-eutectoid alloys is displayed in Fig. 2. At the bottom of the melt almost no specific solidification structure can be found. Higher in the melt pool a cellular structure is found, which transforms to dendrites with side arms.

At higher scan velocities the dendrites in the upper areas no longer have side arms, and cellular like structures are found. Between the cells or dendrites eutectic material is found consisting of Si plates in Al (Fig. 3). Especially at higher velocities, unmelted Si particles are found in the bottom of the melt.

In Al-12Si the solidification structure at low velocities (0.1 cm/s) is eutectic. At higher velocities (0.5 cm/s) some small cells can be observed. These are found to be dendrites which become larger with rising velocity, eventually filling most of the melt bath apart from a small area at the bottom, where the solidification velocity is lower. At these velocities (20cm/s) the dendrites are evolving to cells (Fig. 4).

In Al-20Si large areas with pure Si are found at the bottom of the melt pool. The remaining part of the melt bath has a very fine eutectic structure (Fig. 5), with concentrations at some places of small cells, apparently homogeneously grown in the melt.

For Al-7Si the concentration Si from bottom to top of the melt was determined using EDS. A spot size of 15 μm was used measuring over a large number of solidification structures. At the bottom of the melt a low concentration of Si was found of a few percents. In the rest of the melt bath the average Si concentration rises to a constant level around 8 ± 3 wt%. At velocities above 1 cm/s the concentration profile in the melt bath is constant.

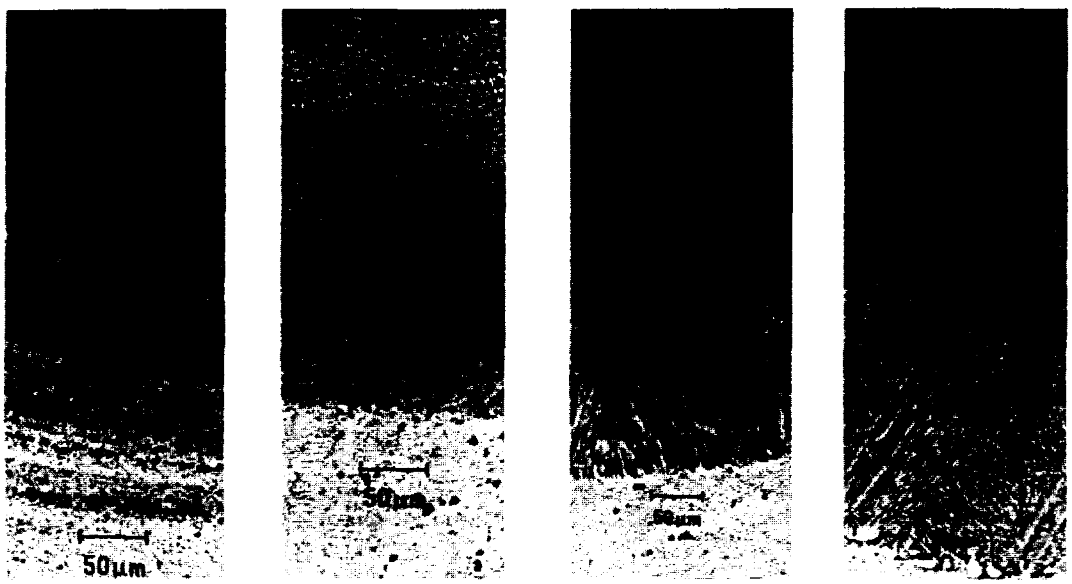

a b c d

Fig. 4 *Solidification structure of Al-12Si at various velocities*
a: *0.2 cm/s,* **b**: *0.5 cm/s,* **c**: *2cm/s,* **d**: *10 cm/s.*

Fig. 5 *Eutectic structure in Al-20Si.*

Theoretical Concepts

Temperature field

Due to the complexity of the laser melting process it is almost impossible to describe it in analytical terms, which is the reason that many authors have worked on different numerical models [10-14].

In numerical models a rectangular grid is chosen with or without varying grid size or with an elliptical co-ordinate system. In every unit volume the incoming and outgoing heat fluxes and the change in temperature from this are calculated. In melting a pure solid at a specific temperature, the latent heat (L) should be supplied, which gives a discontinuity in the temperature-time diagram. To avoid this singularity, we have calculated for each volume the energy of the unit volume and from this the temperature.

For the volume i,j around point y_i, z_j the finite difference equation used was:

$$\frac{\Delta H_{i,j}(T)}{\Delta t} = \frac{\lambda}{\delta^2}((T_{i-1,j} - T_{i,j}) - (T_{i+1,j} - T_{i,j})$$

$$+ (T_{i,j-1} - T_{i,j}) - (T_{i,j+1} - T_{i,j}))$$

$H_{ij}(T)$ = enthalpy at i,j, δ = grid size.

In the present work a cubic grid was chosen with dimension δ. A fully explicit scheme was used and to avoid instabilities the time step Δt was chosen to fulfil the condition $\Delta t < \delta^2/2a$ [15], where a represents the thermal diffusitivity.

Applying the rule of mixtures we took the thermal conductivity as

$$\lambda = f_s \lambda_s + (1 - f_s)\lambda_l$$

f_s = fraction solid, λ_s = thermal conductivity solid and λ_l = thermal conductivity liquid. No undercooling effects were taken into account [16].

Solidification Structures

Solidification may occur with different structures of the solidification front such as: planar, cellular (no relation between growth direction and crystallographic orientation), dendritic (grown in a crystallographic direction) and lamellar or rod like eutectic (two solid phases co-operatively formed) [17-19].

A rigorous treatment of constitutional supercooling, the cause for the formation of particular solidification structures, by Mullins and Sekerka [20], including diffusion around the perturbations and interfacial energy effects, gives the upper and lower limit for non planar growth. Although the prediction of the stability limits is fairly accurate, the theory does not predict which type of pattern is formed at the front and what the size of it will be. Cellular like structures are found near the stability limits and dendrites further away from these limits [21], although there is no sharp distinction between them.

Theories of the dendritical growth behaviour are grouped into three categories: one assumes that dendrites grow at minimum undercooling of the tip [18,22], another assumes that marginal stability concepts determine the tip characteristics [21,23] and a third supposes that the cellular shape is deducible from minimizing the rate of entropy production [24]. Comparison between theory and experiment has not yet been conclusive [25]. By means of the minimum undercooling criterion, the tip temperature and primary arm spacing can be calculated [26,18].

When two phases are growing simultaneously, an eutectic structure is formed. The solidification front is essentially flat. If there is a large difference between the concentration of the phases a rod like structure is more likely to form, in the other case a lamellar or flake type of structure is formed. In regular eutectics no phase has a high entropy of fusion, in irregular eutectics at least one phase has a high entropy of fusion, i.e. it is capable of faceting (Si in Al-Si alloys), giving rise to faceted rods or for higher concentrations either flakes or lamellar structures with varying lamelar distances between the faceting phase [27]. Eutectic structures are formed because, due to the relatively small inter-lamellar distances and the plane front, lateral solute redistribution is rather easy and solidification can occur with a small undercooling. Jackson and Hunt [28] treated eutectic formation theoretically.

For very high solidification velocities an extension is made [30] which indicates that at those velocities (50 cm/s for Al-Cu alloys) larger undercooling should be expected and eventually no eutectic is formed any more. Measurements on Al-Si equilibrium eutectic concentration gave as undercooling [31].

$$T_t = T_L - \xi\sqrt{\frac{V_s}{G}}$$

where $\xi = 1.10^5 m^{-1} s^{1/2} K^{3/2}$.

Although the accuracy of this relation is relatively low it is remarkable that one of the parameters is G the temperature gradient in spite of other measurements on irregular eutectics [29]. To find out which structure is to be expected during solidification one can apply the criterion of minimal undercooling of the solidification front.

Discussion

For the different concentrations used numerical simulations of the temperature behaviour were made using the scheme as described before at a velocity of 10 cm/s. The form and depth of the profiles were in reasonable agreement with the measurements using an absorption of 20% comparable with results of [16]. The solidification velocity at the bottom is almost 0 and it increases rapidly towards the center of the surface of the melt bath. The gradient is in the order of 1.10^6 K/m at the bottom of the melt bath, increases somewhat to $3\text{-}10 \cdot 10^6$ at one third of the depth and decreases further toward the surface.

The lower limit of stability of a planar wave front lies in the order of 20 μm/s, which means that it is almost immediately surpassed after solidification has started. The upper limit lies in the order of 50 m/s. It indicates that most of the solidification occurs in the dendritical regime and areas without solidification structure or a vaguely banded structure are less likely to occur [32].

We used these values to calculate the undercooling and the primary arm spacing for dendrites/cells applying the marginal stability and minimum undercooling criteria and the undercooling for eutectic formation. Both theories for dendritic/cellular growth predict a decrease with velocity of the primary arm spacing as is experimentally confirmed. The other predictions from the marginal stability model were not confirmed by the measurements: undercooling of a few hundred K occurred and dendrite tip radii and primary arm distances were found. The minimum undercooling model gave much better agreement: primary spacings in the order of micrometers and under-coolings in the order of 10 K are found.

For 12.6 wt% Si alloy at low velocities the undercooling for dendrite formation is calculated to be larger than for the forming of eutectic material, however, at larger velocities it is more likely that cells and dendrites occur, as was indeed found to be the case (Fig. 4). Also the formation of eutectic material at 20 wt% Si could be explained from the calculated undercooling temperatures (Fig. 5): being much larger for the formation of Al or Si dendrites than for eutectic type of solidification.

The differences between both theories for predicting the eutectic formation were rather small but the Jackson and Hunt model together with the minimum undercooling criterion described the occurrence of dendrites better despite the fact that for an irregular eutectic this model is rather crude due to the fact that not a single lamellar spacing is found but a certain range.

Conclusions

In laser treated Al-Si alloys (between 4 wt% and 20 wt% Si) the hypo-eutectoid alloys showed Al dendrites surrounded by flake like eutectic material. In the eutectic material a transition occurred from eutectic type of solidification (low velocity) to dendritical solidification (velocities above 10 cm/s). In hyper-eutectoid 20 wt% Si alloy mainly lamellar eutectic type of solidification was found.

A comparison of these results with modern solidification theory using the criteria of marginal stability and minimum undercooling, indicates that only the last one predicts the size of dendrites/cells adequately.

The occurrence of dendrites in eutectic material and of eutectic type in the 20 wt% Si alloy can be predicted using the minimum undercooling criterion and either the empirical relation for undercooling or the Jackson and Hunt relation.

Acknowledgements

This work is part of the research program of the Foundation for Fundamental Research on Matter (FOM-Utrecht) and has been made possible by financial support from the Netherlands Organization for Research (NWO-The Hague).

References

[1] H. J. Hegge, J. Th. M. De Hosson: Proc. 2nd. Europ. Conf. Laser Treatment of Materials, Bad Nauheim, FRG, 13-14 Oct. 1988, DVS, bnd. 113, pp 160-163.

[2] M. Wu, Z. Jin, W. Wu: Werkstoffe & Korrosion, 1987, **38**, pp 124-128.

[3] H. Haddenhorst, E. Hornbogen, H. W. Vollmer: Proc. 2nd. Europ.Conf. Laser Treatment of Materials, Bad Nauheim, FRG, 13-14 Oct. 1988, DVS, bnd. 113, pp 97-99.

[4] W. Kurz, D. J. Fisher: Fundamentals of Solidification (Switzerland, 1985) Trans. Tech. Publ., 2nd print.

[5] W. Kurz, R. Trivedi: Proc. 2nd. Europ. Conf. Laser Treatment of Materials, Bad Nauheim, FRG, 13-14 Oct. 1988, DVS, bnd. 113, pp 92-94.

[6] T. Zacahria, S. A. David, J. M. Vitek, T. Debroy, Met. Trans. **20A**, 957 (1989).

[7] V. Laxmanan: Acta Metall., 1985, **33**, pp 1023-1035.

[8] P. A. Molian: J. Mat. Sci. Lett., 1985, **4**, pp 265-267.

[9] K. A. Jackson, G. H. Gilmer, H. J. Leamy: Proc. Conf. Laser and Electron Beam Processing of Materials, Cambridge, Mass, USA, 27-30, Nov. 1979 (London 1980) Academic Press, pp 104-110.

[10] M. F. Ashby, K. E. Easterling: Acta. Metall., 1984, **32**, pp 1935-1948.

[11] C. P. Grigoropoulos, R. H. Buckholz, G. A. Domoto: J. Appl. Phys, 1986, 60, pp 2304-2309.

[12] H. E. Cline, T. R. Anthony: J. Appl. Phys., 1977, **48**, pp 3895-3900.

[13] C. Chan, J. Mazumder, M. M. Chen: Met. Trans A, 1984, **15A**, pp 2175-2184.

[14] S. Kou, Y. H. Wang: Met. Trans A, 1986, **17A**, pp 2265-2270.

[15] H. S. Carslaw, J. C. Jaeger: Conduction of Heat in Solids (Oxford, 1959) Clarendon Press, 2nd ed., pp 266-270.

[16] B. Carrupt, A. F. A. Hoadley, M. Rappaz: Proc. 2nd. Europ. Conf. Laser Treatment of Materials, Bad Nauheim, FRG, 13-14 Oct. 1988, DVS, bnd. 113, pp 151-153.

[17] W. A. Tiller, K. A. Jackson, J. W. Rutters, B. Chalmers: Acta Met., 1953, **1**, pp 428-437.

[18] V. Laxmanan: Acta Metall., 1985, **33**, pp 1037-1049.

[19] R. Trivedi: J. Cryst. Growth, 1980, **49**, pp 219.

[20] W. W. Mullins, R. F. Sekerka: J. Appl. Phys., 1964, **35**, pp 444-451.

[21] R. Trivedi: Met. Trans. A, 1984, **15A**, pp 977-982.

[22] M. H. Burder, J. D. Hunt: J. Cryst. Growth, 1974, **22**, pp 109-116.

[23] W. Kurz, D. J. Fisher: Acta Metall., 1981, **29**, pp 11-20.

[24] J. S. Kirkaldy: Scripta Metall., 1980, **14**, pp 739-744.

[25] S. N. Tewari: Met. Trans. A, 1986, **17A**, pp 2279-2290.

[26] W. Kurz, B. Giovanola, R. Trivedi: Acta Metall., 1986, **34**, pp 823-830.

[27] R. Elliot: Mat. Sci. & Eng., 1984, **65**, pp 85-92.

[28] K. A. Jackson, J. D. Hunt: Trans. Met. Soc. AIME, 1966, **236**, pp 1129-1142.

[29] H. Jones, W. Kurz: Z. Metallkde, 1981, **72**, pp 792-797.

[30] R. Trivedi, P. Magnin, W. Kurz: Acta Metall., 1987, **35**, pp 971-980.

[31] B. Tolui, A. Hellawell: Acta Metall., 1976, **24**, pp 565-573.

[32] W. J. Boëttinger, D. Shechtman, R. J. Schaeffer, F. S. Biancaniello: Met. Trans. A, 1984, **15A**, pp 55-66.